

21 **Efficacy of a resveratrol nanoformulation based on a commercially available liposomal**
22 **platform**

23 Carla Caddeo ^{a,*}, Daniela Lucchesi ^b, Xavier Fernàndez-Busquets ^{c,d}, Donatella Valenti ^a, Giuseppe
24 Penno ^b, Anna Maria Fadda ^a, Laura Pucci ^{e,*}

25
26 ^a Dept. of Scienze della Vita e dell'Ambiente, Sezione di Scienze del Farmaco, University of
27 Cagliari, Via Ospedale 72, 09124 Cagliari, Italy

28 ^b Dept. of Clinical and Experimental Medicine, Section of Diabetes and Metabolic Diseases,
29 University of Pisa, via Piero Trivella, 56124 Pisa, Italy

30 ^c Nanomalaria Group, Institute for Bioengineering of Catalonia (IBEC), The Barcelona Institute of
31 Science and Technology, Baldiri Reixac 10-12, Barcelona E08028, Spain

32 ^d Barcelona Institute for Global Health (ISGlobal), Hospital Clínic-Universitat de Barcelona,
33 Rosselló 149-153, Barcelona E08036, Spain

34 ^e Institute of Agricultural Biology and Biotechnology, CNR Pisa, Via Moruzzi 1, 56124 Pisa, Italy

35
36
37 * Corresponding authors:

38 Carla Caddeo

39 Dept. of Scienze della Vita e dell'Ambiente, Sezione di Scienze del Farmaco, University of
40 Cagliari, Via Ospedale 72, 09124 Cagliari, Italy

41 Tel.: +39 0706758462; fax: +39 0706758553; e-mail address: caddeoc@unica.it

42
43 Laura Pucci

44 Institute of Agricultural Biology and Biotechnology, CNR Pisa, Via Moruzzi 1, 56124 Pisa, Italy

45 Tel.: +39 0503153084; e-mail address: laura.pucci@ibba.cnr.it

46 **ABSTRACT**

47 Scalability is one of the important factors slowing down or even impeding the clinical translation of
48 nanoparticle-based systems. **The latter** need to be manufactured at a high level of quality, with
49 batch-to-batch reproducibility, and need to be stable after the manufacturing process, during long-
50 term storage and upon clinical administration. In this study, a vesicular formulation intended for
51 cutaneous applications was developed by the easy reconstitution of a commercially available
52 liposomal **platform. Resveratrol, a naturally occurring compound with potent antioxidant activity,**
53 **and Tween80, a hydrophilic non-ionic surfactant, were included in the formulation.** The physico-
54 chemical properties of the vesicles were assessed using light scattering and cryogenic transmission
55 electron microscopy. Nanosized (around 80 nm) spherical and elongated, unilamellar vesicles were
56 produced, with remarkable storage stability. The incorporation of resveratrol in the vesicular system
57 did not alter its strong antioxidant activity, as demonstrated by antioxidant **colorimetric** assays
58 (DPPH and FRAP). Furthermore, the resveratrol liposomes were cytocompatible with fibroblasts
59 and capable of protecting skin cells from oxidative stress by reducing both endogenous and
60 **chemically** induced reactive oxygen species more effectively than free resveratrol. Therefore, the
61 proposed formulation, based on the use of a commercially available liposomal platform, represents
62 an easy-to-prepare, reproducible, up-scaled and efficient means of delivering resveratrol and
63 potentiating its biological activity *in vitro*.

64

65

66

67

68 **Keywords:** resveratrol; commercial liposomes; skin delivery; skin cells; antioxidant.

69

70 **1. Introduction**

71 New strategies, accessible approaches and technologies are still needed to develop safe and
72 successful therapies. Many untapped and potentially therapeutic molecules with reduced side effects
73 can be found in traditional herbal medicines and foods (Liu, 2013; Pan et al., 2013; Veselkov et al.,
74 2019). Natural compounds such as resveratrol have attracted significant interest in the
75 pharmaceutical research due to their numerous health-promoting effects, coupled with their safety
76 profiles and natural origins (Caddeo et al., 2015; Salehi et al., 2018). Unfortunately, the beneficial
77 use of resveratrol's biological activities is hampered by its low aqueous solubility, chemical
78 instability and rapid metabolism (Ahmadi and Ebrahimzadeh, 2020; Gligorijević et al., 2021). The
79 incorporation of such compounds into liposomes is a well-known and effective approach to
80 overcoming such limitations, with a consequent enhancement of the bioavailability of the payload
81 (Daraee et al., 2016; Lee, 2020).

82 Liposomes are the most successful commercial **nanosized** drug delivery system. They were the first
83 nanoparticle-based system to get regulatory approval for clinical use, and are still the most widely
84 used platform for marketed pharmaceutical products, as well as the best-investigated platform in
85 clinical trials and academic research (Sercombe et al., 2015; Zylberberg and Matosevic, 2016;
86 Nisini et al., 2018; Jensen and Hodgson, 2020).

87 One of the important factors slowing down or even impeding the clinical translation of
88 nanoparticle-based systems is the scalability of the formulations. Platforms that require complex
89 and/or laborious production procedures generally have limited clinical translation potential, as they
90 can be problematic to manufacture on a large scale (Hua et al., 2018). Besides the need for large,
91 scalable quantities, formulations need to be manufactured at a high level of quality, with batch-to-
92 batch reproducibility, and need to be stable after the manufacturing process, during long-term
93 storage and upon clinical administration.

94 As already described, liposomes have been successfully developed on an industrial scale, without
95 the need for multiple manufacturing steps or the use of organic solvents (Jaafar-Maalej et al., 2012;
96 Kraft et al., 2014). Challenges arise when liposome systems become more complex, as the presence
97 of multiple components inevitably poses manufacturing and production problems, increases costs,
98 and makes quality assurance and quality control evaluation more difficult (Svenson, 2012; Tinkle et
99 al., 2014). They may also lead to significant changes in the physico-chemical properties,
100 pharmacokinetic profiles, and pharmacodynamic interactions (Hua et al., 2018). Hence, a balance
101 between the complexity of the formulation design, the therapeutic efficacy and the clinical
102 translation is needed.

103 In light of these considerations, in this study, we have developed a novel vesicular formulation
104 using a commercially available liposomal platform, which is produced on a large scale and which
105 meets quality, safety and reproducibility requirements. The vesicular formulation was optimised for
106 the loading and delivery of resveratrol and characterised to assess its main physico-chemical and
107 technological properties. Additionally, the biocompatibility and antioxidant activity of the
108 resveratrol formulation were investigated in skin cells, with the purpose of assessing the enhanced
109 efficacy of the vesicular delivery.

110

111 **2. Materials and methods**

112 *2.1. Materials*

113 Pronanosome LIPO-N ready-to-use powder vesicles were kindly provided by Nanovex
114 Biotechnologies SL (Llanera, Spain). Tween 80 was purchased from Galeno (Carmignano, Prato,
115 Italy); resveratrol (RSV) and all other reagents, if not otherwise specified, were purchased from
116 Sigma-Aldrich/Merck (Milan, Italy).

117

118 *2.2. Vesicle preparation and characterisation*

119 Resveratrol (2 mg/ml) and Tween 80 (10 mg/ml) were weighed in a ready-to-use glass vial
120 containing Pronanosome LIPO-N in its dried form (100 mg) and dispersed in water (2 ml; Table 1).
121 To reconstitute the vesicles, the dispersion was hand-shaken, left to hydrate overnight and sonicated
122 (5 sec on and 2 sec off, 20 cycles; 13 microns of probe amplitude) with a Soniprep 150 (MSE
123 Crowley, London, UK).

124 For comparative purposes, empty vesicles were prepared following the above procedure, but
125 without the addition of resveratrol (Table 1).

126 All the samples were prepared and kept in the dark for the duration of the experiments.

127 Vesicle formation and morphology were examined using cryogenic-transmission electron
128 microscopy (cryo-TEM). For the analysis, a thin aqueous film was formed by placing 5 μ l of the
129 vesicular dispersion on a glow-discharged holey carbon grid and then blotting the grid against filter
130 paper. The resulting thin sample film spanning the grid holes was vitrified by plunging the grid
131 (kept at 100% humidity and room temperature) into ethane, maintained at its melting point with
132 liquid nitrogen using a Vitrobot (FEI Company, Eindhoven, The Netherlands). The vitreous film
133 was transferred to a Tecnai F20 TEM (FEI Company) using a Gatan cryo-transfer (Gatan,
134 Pleasanton, CA, US), and the sample was observed in a low-dose mode. Images were acquired at
135 200 kV at a temperature of $-170/-175$ °C, using low-dose imaging conditions not exceeding $20 e^-$
136 $/\text{\AA}^2$, with a 4096×4096 pixel CCD Eagle camera (FEI Company).

137 The average diameter, polydispersity index (PI, a measure of the width of size distribution) and zeta
138 potential of the vesicles were determined via dynamic and electrophoretic light scattering using a
139 Zetasizer nano-ZS (Malvern Panalytical, Worcestershire, UK). Samples ($n > 6$) were diluted with
140 water (1:100) and analysed at 25 °C.

141 The **vesicle dispersions** were purified from the non-incorporated resveratrol by dialysis. Each
142 sample (1 ml) was loaded into Spectra/Por[®] tubing (12–14 kDa MW cut-off; Spectrum Laboratories
143 Inc., DG Breda, The Netherlands), previously rinsed in water, and dialysed against water (2 l) for 2

144 h to allow the removal of the non-incorporated **resveratrol**. After disruption of unpurified and
145 purified vesicles with methanol, the entrapment efficiency (E), expressed as the percentage of the
146 amount of resveratrol **detected in unpurified samples**, was determined by high performance liquid
147 chromatography (Alliance 2690, Waters, Milan, Italy). Resveratrol content was assayed using a
148 XSelect C18 column (3.5 μm , 4.6 \times 150 mm, Waters), with a mobile phase consisting of methanol,
149 acetonitrile, water and acetic acid (75:22.5:2.4:0.1, v/v) at a flow rate of 0.8 ml/min. A₃₀₆ was
150 measured for resveratrol quantification.

151 **The stability of the formulations was evaluated by monitoring vesicle mean size, PI, zeta potential**
152 **and resveratrol content over three months at 4 ± 2 °C.**

153

154 *2.3. Antioxidant activity: DPPH and FRAP assays*The antioxidant activity of the resveratrol
155 formulations was assessed by evaluating their ability to scavenge 2,2-diphenyl-1-picrylhydrazyl
156 (DPPH), a stable nitrogen-centered free radical. DPPH was dissolved in methanol to yield a 25 μM
157 concentration, and the solution (2 ml) was mixed with 20 μl of each sample (i.e., empty vesicles,
158 resveratrol vesicles, resveratrol methanolic solution), and stored at room temperature for 30 min, in
159 the dark. Thereafter, the absorbance was measured at 517 nm against blank. The extent of
160 discoloration of the violet colour of DPPH methanolic solution, quantified as a decrease in
161 absorbance, depends on the intrinsic antioxidant activity/radical scavenging activity and
162 concentration of a sample. Antioxidant compounds can neutralize the DPPH radical by either direct
163 reduction via electron donation or by radical quenching via hydrogen atom donation. The DPPH
164 radical scavenging activity of each sample was expressed as (i) percent antioxidant activity (AA)
165 calculated according to the following formula, where A is the absorbance:

166
$$AA = \left(\frac{A_{DPPH} - A_{sample}}{A_{DPPH}} \right) \times 100$$

167 and (ii) as Trolox equivalent antioxidant capacity (TEAC). The TEAC values were calculated based
168 on a calibration curve plotted using Trolox (reference standard) at different concentrations (0.1–1
169 mg/ml). Results were expressed as mg Trolox equivalents/ml solution. TEAC reflects the ability of
170 antioxidant samples to scavenge DPPH radical as compared with that of Trolox: the higher the
171 TEAC values, the higher the radical scavenging activity of the samples.

172 The antioxidant activity was also assessed by the FRAP (ferric reducing antioxidant power) assay,
173 which evaluates antioxidants as reductants of Fe^{3+} to Fe^{2+} : Fe^{3+} is chelated by 2,4,6-tris(pyridin-2-
174 yl)-1,3,5-triazine (TPTZ) to form a Fe^{2+} -TPTZ blue-coloured complex that increases the absorption
175 at 593 nm (Tuberoso et al., 2013). A ferric complex solution was freshly prepared with TPTZ and
176 Fe^{3+} (0.3123 g TPTZ, 0.5406 g $\text{FeCl}_3 \cdot 6\text{H}_2\text{O}$ in 100 ml acetate buffer pH 3.6). 20 μl of each sample
177 (i.e., empty vesicles, resveratrol vesicles, resveratrol methanolic solution) was dissolved in 2 ml of
178 the ferric complex solution and incubated for 4 min in the dark; absorbance at 593 nm was
179 measured with a spectrophotometer. Quantitative analysis was performed according to the external
180 standard method (FeSO_4 , mg/ml), correlating the absorbance of the samples with the FeSO_4
181 concentration, and results were expressed as ferrous equivalents (mg Fe^{2+} equivalents (FE)/ml
182 solution).

183

184 2.4. Fibroblast cell culture

185 3T3-L1 cells (ATCC[®]CL-173TM) were grown in Dulbecco's modified Eagle's medium (DMEM)
186 supplemented with 10% fetal bovine serum (FBS), 100 units/ml penicillin, and 100 $\mu\text{g}/\text{ml}$
187 streptomycin, and maintained at 37 °C in a humidified 5% CO_2 incubator. The cells were seeded
188 into 96-well plates and tested under the following experimental conditions:

189 1. cells unexposed (control) or exposed to 250 μM 2,2'-azobis(2-methylpropionamide)
190 dihydrochloride (AAPH, a peroxy radical generator used as a positive control) for 4 h;

191 2. cells exposed to resveratrol liposomes or resveratrol ethanolic solution, previously diluted to
192 reach the required doses of resveratrol (0.01, 0.1, 1.0 and 10 $\mu\text{g}/\text{well}$), for 5 h;
193 3. cells exposed to resveratrol liposomes or resveratrol ethanolic solution, previously diluted to
194 reach the required doses of resveratrol (0.01, 0.1, 1.0 and 10 $\mu\text{g}/\text{well}$), for 1 h and co-incubated with
195 250 μM AAPH for a further 4 h. For comparative purposes, empty liposomes were tested at the
196 same dilutions as the resveratrol liposomes or ethanolic solution.

197

198 *2.5. Assessment of viability*

199 The MTT assay was performed to evaluate the viability of cultured 3T3-L1 cells upon different
200 treatment conditions (see Section 2.4). MTT (3-(4,5-dimethylthiazol-2-yl)-2,5-diphenyltetrazolium
201 bromide) reagent (Sigma, St. Louis, MO, USA) measures mitochondrial activity in live cells.
202 Briefly, fibroblasts (5×10^4 cells/well) were incubated with MTT (0.5 mg/ml) for 3 h at 37 °C in 5%
203 CO₂. After incubation, the medium was removed, and the cells solubilised in 10% DMSO/90%
204 isopropanol. Then, the amount of the dye released from the cells was quantified by measuring the
205 optical density at 540 nm (reference wavelength: 620 nm) by using a multiplate reader (Multiskan
206 EX, Thermo Fisher Scientific, Waltham, MA, US). The experiment was repeated at least three
207 times independently, each time in triplicate.
208 Results are expressed as percentage *vs.* control cells viability.

209

210 *2.6. Assessment of cellular reactive oxygen species (ROS)*

211 After incubation of 3T3-L1 cells with the samples or the samples and 250 μM AAPH (see Section
212 2.4), endogenous or chemically-induced cellular ROS were detected using 5-(and-6)-chloromethyl-
213 2',7'-dichlorodihydrofluorescein diacetate, acetyl ester (CM-H₂DCF-DA; Invitrogen, Life
214 Technologies Ltd, Thermo Fisher Scientific, Waltham, MA, US) fluorescent probe.

215 Briefly, 3T3-L1 cells, seeded at a density of 5×10^4 cells/well into a 96-well blackened fluorescence
216 plate, were incubated with CM-H₂DCF-DA (5 μ M/well) for 60 min at 37 °C in the dark.
217 Afterwards, the cells were rinsed with 1 \times PBS to remove CM-H₂DCF-DA solution and treated
218 according to the experimental conditions reported in Section 2.4.

219 ROS production was detected by measuring fluorescence intensity at 485 nm excitation and 520 nm
220 emission using a FLUOstar[®] Omega multi-mode microplate reader. The fluorescence plate reader
221 measures the light signal emitted by a sample in Relative Fluorescent Units (RFU). The experiment
222 was repeated at least three times independently, each time in triplicate. Results are expressed as
223 percentage vs. control cells ROS production.

224 3T3-L1 cells (CTR), untreated or incubated with 250 μ M AAPH, or co-incubated with 250 μ M
225 AAPH and empty liposomes, resveratrol solution, resveratrol liposomes for 5 h were examined
226 under a Primo Vert inverted microscope (Carl Zeiss Microscopy GmbH, Jena, Germany) to assess
227 cell morphology.

228

229 *2.7. Statistical analysis of data*

230 Results are expressed as the mean \pm standard deviation (SD). Statistical analysis of data was
231 performed using StatView software package (SAS Institute Inc., Cary, NC, US) by one-way
232 analysis of variance (ANOVA). Fisher's post-hoc test was used for single comparisons. *P* values
233 <0.05 were considered as statistically significant.

234

235 **3. Results and discussion**

236 *3.1. Vesicle design and characterization*

237 The present study was aimed at developing a vesicular formulation for the delivery of resveratrol to
238 the skin. A commercial liposomal platform, Pronanosome LIPO-N, was used for the preparation of
239 small, reproducible, and stable liposomes. Given their versatility and ease of use, Pronanosome

240 LIPO-N can be loaded with any bioactive compound. In this work, Pronanosome LIPO-N were
241 loaded with resveratrol, a natural polyphenol with countless biological activities.

242 In order to discriminate between the effect of the carrier and the polyphenol, resveratrol liposomes
243 were prepared, characterised and tested *in vitro* in comparison with empty liposomes.

244 Light scattering results, summarised in Table 2, showed that empty liposomes were small in size
245 (~80 nm). **These liposomes were also characterized by** high homogeneity (PI 0.22), and negative
246 zeta potential (-25 mV), due to the charge carried by the proprietary **Pronanosome LIPO-N**
247 phospholipid mixture. The loading of resveratrol did not alter these values ($p>0.05$), **with the**
248 **exception of** the PI value, which was lower (0.19; $p<0.05$). **This finding was** indicative of an even
249 higher homogeneity of the vesicle formulation.

250 The entrapment efficiency of the liposomes was high (83%; Table 2), and the amount of the loaded
251 resveratrol did not diminish during a **three-month-** storage period ($p>0.05$). This **aligns** with
252 previous results showing that resveratrol is efficiently loaded in phospholipid vesicles (Caddeo et
253 al., 2018; Caddeo et al., 2021).

254 Cryo-TEM observation of resveratrol liposomes confirmed the formation of small unilamellar
255 vesicles, **either** spherical or elongated (Fig. 1); no evidence of free resveratrol crystals **was seen**.

256 **As known**, the stability of a nanoparticle-based formulation is critical to ensure its **use is both** safe
257 and effective. The stability of the resveratrol formulation was evaluated by monitoring the mean
258 diameter, PI and zeta potential of the vesicles over three months of storage. As the results show in
259 Fig. 2, no significant variations **were found among** the three examined parameters ($p>0.05$).

260

261 3.3. Antioxidant assays

262 **Antioxidant** activity of the resveratrol formulation was assessed by evaluating its ability to scavenge
263 radical species (DPPH assay) and reduce ferric ions (FRAP assay).

264 The DPPH assay exploits the reduction of the DPPH free radical in the presence of antioxidant
265 molecules **such as** resveratrol. The results of the assay are summarised in Table 3. The DPPH
266 radical was almost completely scavenged (87%). Given the strong antioxidant power of resveratrol,
267 **this was expected. It is worth noting that** the antioxidant activity of resveratrol in liposomes was
268 **essentially** the same (84%; $p>0.05$), corresponding to ~320 µg/ml of Trolox equivalents. **This**
269 **demonstrated that** incorporation in the vesicle system did not alter the inner properties of the
270 polyphenol.

271 The FRAP assay exploits the reduction of Fe^{3+} by antioxidant molecules. The results obtained from
272 the assay showed the same trend; **the** resveratrol liposomes displayed a **reduction** potential as strong
273 as that of free resveratrol, **which was** around 8 mg/ml of ferrous equivalents (Table 3). These
274 findings confirm that the antioxidant activity of resveratrol was retained in the vesicle formulation.

275

276 3.4. Cell viability

277 To assess the effect of the vesicular formulation on 3T3-L1 fibroblasts, we evaluated cell viability
278 in **both** the presence **and** absence of AAPH-induced oxidative stress. **3T3-L1 fibroblasts were**
279 **incubated with 0, 100, 250, 500 and 1000 µM AAPH for 4 h, and the concentration that triggered**
280 **ROS production without significantly reducing cell viability was determined.** Given the results
281 reported in Fig. 3, **it was shown** that 100 µM AAPH did not reduce cell viability. **However,** 500 and
282 1000 µM AAPH **concentrations were too strong, and they resulted in a 30% mortality rate. A proper**
283 **concentration of 250 µM AAPH was selected** for the assessment of cell viability and intracellular
284 ROS production under stress conditions.

285 The absence of cytotoxic effects of the formulations was evaluated in 3T3-L1 fibroblasts in terms of
286 viability. **This followed 5 h of** exposure to increasing doses of resveratrol ranging from 0.01 to 10
287 µg (Fig. 4). Analysis of variance showed a significant difference between groups after 5 h exposure
288 ($p<0.0001$). After this time, cytotoxicity was significantly induced by the higher **testing** dose of

289 resveratrol solution (10 µg; $p < 0.0001$ vs. control); **this resulted in a mortality rate** of 82.1%. Such
290 decrease in viability was prevented by liposomes; the mortality **rate** of cells exposed to resveratrol
291 liposomes (10 µg; $p < 0.0001$ vs. control) was 55%. The protection offered by the nanocarrier was
292 confirmed by the low mortality (27.4%; $p = 0.0144$ vs. control) of cells exposed to empty
293 liposomes, **which were** tested at the same dilution used to reach 10 µg resveratrol.
294 In **the** presence of 250 µM AAPH, the same behaviour was observed (Fig. 4). Cell viability was
295 significantly reduced only **in the case of** exposure to the higher dose of resveratrol. **This confirmed**
296 the mortality values found under non-stress conditions: 82.3% with resveratrol solution ($p < 0.0001$
297 vs. 250 µM AAPH), 54.4% with resveratrol liposomes ($p < 0.0001$ vs. 250 µM AAPH), and 34.2%
298 with empty liposomes ($p = 0.0024$ vs. 250 µM AAPH).
299 Therefore, the effects of spontaneous and induced oxidative stress were superimposable. The results
300 point to the ability of liposomes to protect the cells from the inner toxicity of high doses of
301 resveratrol **that lead** to cell death. This **aligns** with previous studies showing that resveratrol can act
302 as either an antioxidant or **a** pro-oxidant agent. **Aside** from the treatment conditions, **the** specific
303 microenvironment, **the** type of cells, and their basal redox state, **this depends** on the concentration
304 used (Alarcón de la Lastra and Villegas, 2007; Khan et al., 2013). Dose-dependent effects have
305 been described. At low concentrations, resveratrol acts as an antioxidant that can protect from DNA
306 damage and oxidative stress. At high concentrations, it acts as a pro-oxidant **that promotes** DNA
307 damage and **increases** oxidative stress (Calabrese et al., 2010; Shaito et al., 2020).

308

309 *3.5. Intracellular ROS production*

310 The antioxidant activity of the resveratrol formulation was analysed in AAPH-stressed 3T3-L1 skin
311 cells as **a reducer** of ROS levels. **This was performed** by using DCFH-DA, a cell-permeable dye
312 sensitive to the cellular redox state.

313 A total of 5 h of exposure was performed with resveratrol solution, empty liposomes, and
314 resveratrol liposomes in the absence of AAPH in cell culture. Aside from when cells were incubated
315 with the higher dose of empty liposomes, no increase in spontaneous ROS production was detected
316 (Fig. 5).

317 The incubation of cells with 250 μ M AAPH significantly triggered ROS production (50% increase;
318 $p < 0.0001$ vs. control). The treatment with empty liposomes at higher doses caused a further
319 increase in the cellular ROS levels (Fig. 5). On the other hand, a statistically significant dose-
320 dependent decrease in ROS levels was found upon exposure to resveratrol solution. Similarly, a
321 significant decrease in ROS was observed upon treatment with resveratrol liposomes, which
322 restored the basal levels at the higher dose (10 μ g; $p < 0.0001$ vs. 250 μ M AAPH).

323 The low levels of ROS detected in cells treated with 10 μ g resveratrol solution were seemingly
324 comparable to those detected in untreated control cells (Fig. 5). However, this was not due to the
325 antioxidant activity of resveratrol; the low levels were attributed to the reduced number of live cells.
326 Indeed, as displayed by the viability data reported in Fig. 4, a 10 μ g resveratrol solution caused an
327 82% cell mortality rate. This result was confirmed by the images obtained with an inverted
328 microscope (Fig. 6). It was shown that the application of the higher dose of resveratrol solution in
329 AAPH-exposed cells was clearly associated with a significant cell death. This, in turn, leads to
330 lower ROS levels. However, in terms of morphology and number, it was apparent that cells treated
331 with the same dose of resveratrol liposomes (i.e., 10 μ g) displayed features similar to untreated cells
332 (Fig. 6).

333

334 4. Conclusions

335 The results of the present work demonstrated that the resveratrol formulation developed by using a
336 commercially available liposomal platform ensured the requirements of quality, reproducibility, and

337 efficiency. The liposomes were small in size, highly stable, and effective in preserving the
338 antioxidant activity of resveratrol and reducing its cytotoxicity at high doses.

339 Therefore, these findings respond to the need to develop scalable formulations **characterized by**
340 high quality, **safety**, and **effectiveness**. Further research, such as targeted *in vivo* tests, are needed to
341 validate the *in vitro* potential of the resveratrol formulation for clinical translation.

342

343 **Acknowledgments**

344 The Authors would like to thank Nanovex Biotechnologies SL (Parque Tecnológico de Asturias,
345 CEEI, 33428 Llanera, Asturias, Spain) for kindly providing Pronanosome LIPO-N.

346 This research was partially supported by the following grants: RASSR14371 under FSC 2014-2020
347 program - Patto per lo Sviluppo della Regione Sardegna; RTI2018-094579-B-I00 (Spanish Ministry
348 of Science, Innovation and Universities, Spain), which included FEDER funds; and 2017-SGR-908
349 (Generalitat de Catalunya, Spain).

350 ISGlobal and IBEC are members of the CERCA Programme, *Generalitat de Catalunya*. We
351 acknowledge support from the Spanish Ministry of Science, Innovation and Universities through
352 the “*Centro de Excelencia Severo Ochoa 2019-2023*” Program (CEX2018-000806-S). This
353 research is part of ISGlobal's Program on the Molecular Mechanisms of Malaria which is partially
354 supported by the *Fundación Ramón Areces*.

355

356 **References**

- 357 Liu, R.H., 2013. Dietary bioactive compounds and their health implications. *J. Food Science* 78, S1.
- 358 Pan, S.-Y., Zhou, S.-F., Gao, S.-H., Yu, Z.-L., Zhang, S.-F., Tang, M.-K., Sun, J.-N., Ma, D.-L.,
359 Han, Y.-F., Fong, W.-F., Ko, K.-M., 2013. New perspectives on how to discover drugs from herbal
360 medicines: CAM's outstanding contribution to modern therapeutics. *Evid Based Complement.*
361 *Alternat. Med.* 627375.
- 362 Veselkov, K., Gonzalez, G., Aljifri, S., Galea, D., Mirnezami, R., Youssef, J., Bronstein, M.,
363 Laponogov, I., 2019. HyperFoods: machine intelligent mapping of cancer-beating molecules in
364 foods. *Scientific Reports* 9, 9237.
- 365 Caddeo, C., Manconi, M., Cardia, M.C., Díez-Sales, O., Fadda, A.M., Sinico, C., 2015.
366 Investigating the interactions of resveratrol with phospholipid vesicle bilayer and the skin: NMR
367 studies and confocal imaging. *Int. J. Pharm.* 484, 138-145.
- 368 Salehi, B., Prakash Mishra, A., Nigam, M., Sener, B., Kilic, M., Sharifi-Rad, M., Valere Tsouh
369 Fokou, P., Martins, N., Sharifi-Rad, J., 2018. Resveratrol: a double-edged sword in health benefits.
370 *Biomedicines* 6(3), 91.
- 371 Ahmadi, R., Ebrahimzadeh, M.A., 2020. Resveratrol - A comprehensive review of recent advances
372 in anticancer drug design and development. *Eur. J. Med. Chem.* 200, 112356.
- 373 Gligorijević, N., Stanić-Vučinić, D., Radomirović, M., Stojadinović, M., Khulal, U., Nedić, O.,
374 Ćirković Veličković, T., 2021. Role of resveratrol in prevention and control of cardiovascular
375 disorders and cardiovascular complications related to COVID-19 disease: mode of action and
376 approaches explored to increase its bioavailability. *Molecules* 26, 2834.
- 377 Daraee, H., Etemadi, A., Kouhi, M., Alimirzalu, S., Akbarzadeh, A., 2016. Application of
378 liposomes in medicine and drug delivery. *Artif. Cells Nanomed. Biotechnol* 44, 381–391.
- 379 Lee, M.-K., 2020. Liposomes for enhanced bioavailability of water-insoluble drugs: in vivo
380 evidence and recent approaches. *Pharmaceutics* 12(3), 264.

381 Sercombe, L., Veerati, T., Moheimani, F., Wu, S.Y., Sood, A.K., Hua, S., 2015. Advances and
382 challenges of liposome assisted drug delivery. *Front. Pharmacol.* 6, 286.

383 Zylberberg, C., Matosevic, S., 2016. Pharmaceutical liposomal drug delivery: a review of new
384 delivery systems and a look at the regulatory landscape. *Drug Deliv.* 23(9), 3319–3329.

385 Nisini, R., Poerio, N., Mariotti, S., De Santis, F., Fraziano, M., 2018. The multirole of liposomes in
386 therapy and prevention of infectious diseases. *Front. Immunol.*, 9, 155.

387 Jensen, G.M., Hodgson, D.F., 2020. Opportunities and challenges in commercial pharmaceutical
388 liposome applications. *Adv. Drug Deliv. Rev.* 154–155, 2-12.

389 Hua, S., de Matos, M.B.C., Metselaar, J.M., Storm, G., 2018. Current trends and challenges in the
390 clinical translation of nanoparticulate nanomedicines: pathways for translational development and
391 commercialization. *Front. Pharmacol.* 9, 790.

392 Jaafar-Maalej, C., Elaissari, A., Fessi, H., 2012. Lipid-based carriers: manufacturing and
393 applications for pulmonary route. *Expert Opin. Drug Deliv.* 9, 1111–1127.

394 Kraft, J.C., Freeling, J.P., Wang, Z., Ho, R.J., 2014. Emerging research and clinical development
395 trends of liposome and lipid nanoparticle drug delivery systems. *J. Pharm. Sci.* 103, 29–52.

396 Svenson, S., 2012. Clinical translation of nanomedicines. *Curr. Opin. Solid. State Mater. Sci.* 16,
397 287–294.

398 Tinkle, S., McNeil, S.E., Muhlebach, S., Bawa, R., Borchard, G., Barenholz, Y.C., Tamarkin, L.,
399 Desai, N., 2014. Nanomedicines: addressing the scientific and regulatory gap. *Ann. N. Y. Acad.*
400 *Sci.* 1313, 35–56.

401 Tuberoso, C.I.G., Boban, M., Bifulco, E., Budimir, D., Pirisi, F.M., 2013. Antioxidant capacity and
402 vasodilatory properties of Mediterranean food: The case of Cannonau wine, myrtle berries liqueur
403 and strawberry-tree honey. *Food Chem.* 140, 686-691.

404 Caddeo, C., Pucci, L., Gabriele, M., Carbone, C., Fernández-Busquets, X., Valenti, D., Pons, R.,
405 Vassallo, A., Fadda, A.M., Manconi, M., 2018. Stability, biocompatibility and antioxidant activity
406 of PEG-modified liposomes containing resveratrol. *Int. J. Pharm.* 538, 40–47.

407 Caddeo, C., Gabriele, M., Nacher, A., Fernandez-Busquets, X., Valenti, D., Fadda, A.M., Pucci, L.,
408 Manconi, M., 2021. Resveratrol and artemisinin eudragit-coated liposomes: A strategy to tackle
409 intestinal tumors. *Int. J. Pharm* 592, 120083.

410 Alarcón de la Lastra, C., Villegas, I., 2007. Resveratrol as an antioxidant and pro-oxidant agent:
411 mechanisms and clinical implications. *Biochem. Soc. Trans.* 35, part 5.

412 Khan, A., Chen, H., Wan, X., Tania, M., Xu, A., Chen, F., Zhang, D., 2013. Regulatory effects of
413 resveratrol on antioxidant enzymes: a mechanism of growth inhibition and apoptosis induction in
414 cancer cells. *Mol. Cells* 35, 219-225.

415 Calabrese, E.J., Mattson, M.P., Calabrese, V., 2010. Resveratrol commonly displays hormesis:
416 occurrence and biomedical significance. *Hum. Exp. Toxicol.* 29, 980–1015.

417 Shaito, A., Posadino, A.M., Younes, N., Hasan, H., Halabi, S., Alhababi, D., Al-Mohannadi, A.,
418 Abdel-Rahman, W.M., Eid, A.H., Nasrallah, G.K., Pintus, G., 2020. Potential adverse effects of
419 resveratrol: a literature review. *Int. J. Mol. Sci.* 21, 2084.

420

421

422 **Figure captions**

423 **Figure 1.** Cryo-TEM images of resveratrol liposomes.

424 **Figure 2.** Long-term stability of resveratrol liposomes assessed by monitoring mean diameter
425 (MD), polydispersity index (PI) and zeta potential (ZP) for 90 days.

426 **Figure 3.** Effect of AAPH exposure on 3T3-L1 cells viability. Data are expressed as means \pm SD;
427 $n=3$. ** $p \leq 0.01$ vs. control (i.e., cells + 0 μ M AAPH).

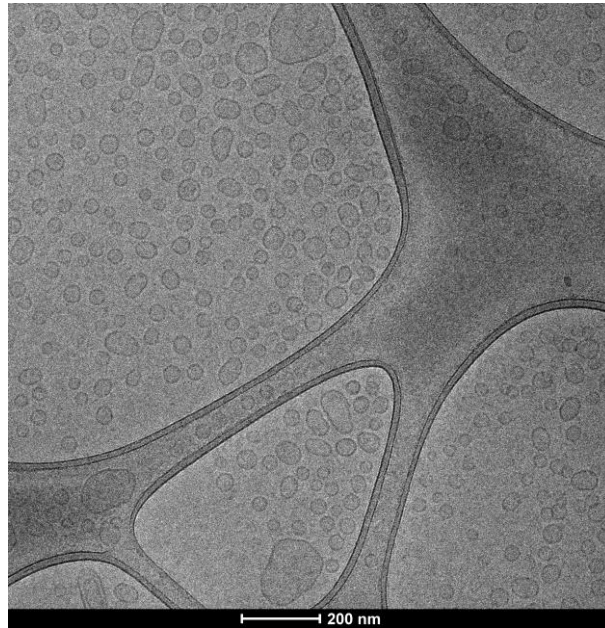
428 **Figure 4.** Cell viability in the absence or presence of oxidative stress induced by AAPH and upon
429 exposure to empty liposomes, resveratrol solution, and resveratrol liposomes for 5 h. Data are
430 expressed as means \pm SD; $n=33$. * $p < 0.05$ vs. control; **** $p < 0.0001$ vs. control; ### $p < 0.005$ vs.
431 250 μ M AAPH; ##### $p < 0.0001$ vs. 250 μ M AAPH.

432 **Figure 5.** Effects of 5 h exposure to empty liposomes, resveratrol solution, and resveratrol
433 liposomes on ROS production in 3T3-L1 cells, in the absence or presence of AAPH induced-
434 oxidative stress. Data are expressed as means of RFU (Relative Fluorescent Units) \pm SD; $n=33$.
435 * $p < 0.05$ vs. control; § $p < 0.0001$ vs. control; # $p < 0.05$ vs. 250 μ M AAPH; ## $p \leq 0.01$ vs. 250 μ M
436 AAPH; ### $p < 0.005$ vs. 250 μ M AAPH; ##### $p \leq 0.0001$ vs. 250 μ M AAPH; □□□ $p \leq 0.0001$ vs. empty
437 liposomes 10 μ g + 250 μ M AAPH; δδδ $p \leq 0.0001$ vs. empty liposomes 1 μ g + 250 μ M AAPH; ζζ
438 $p = 0.0005$ vs. empty liposomes 0.1 μ g + 250 μ M AAPH.

439 **Figure 6.** Representative microscope images of untreated 3T3-L1 cells (CTR), incubated with 250
440 μ M AAPH, or incubated with 250 μ M AAPH and exposed for 5 h to 10 μ g empty liposomes,
441 resveratrol solution, or resveratrol liposomes.

442

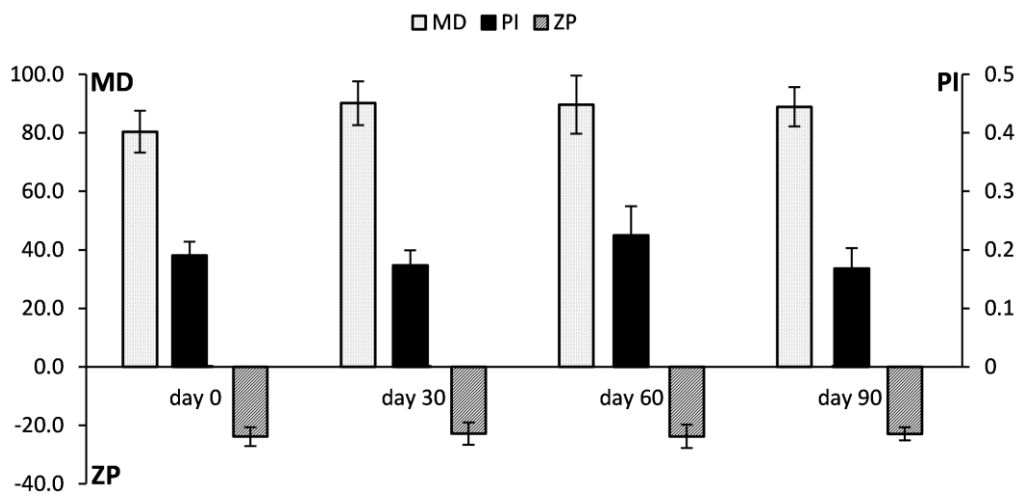
443



444

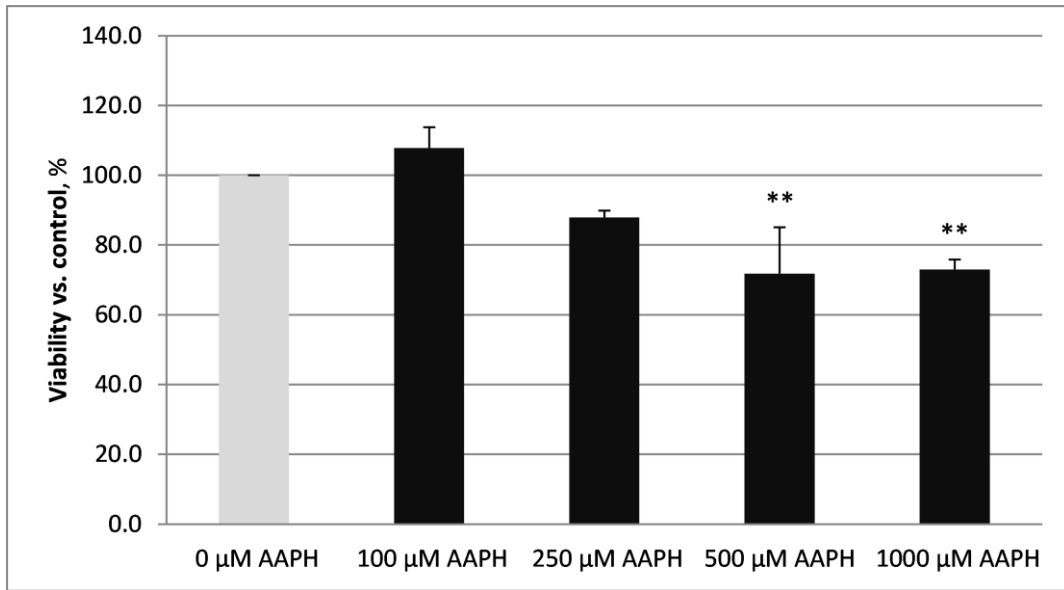
445

446



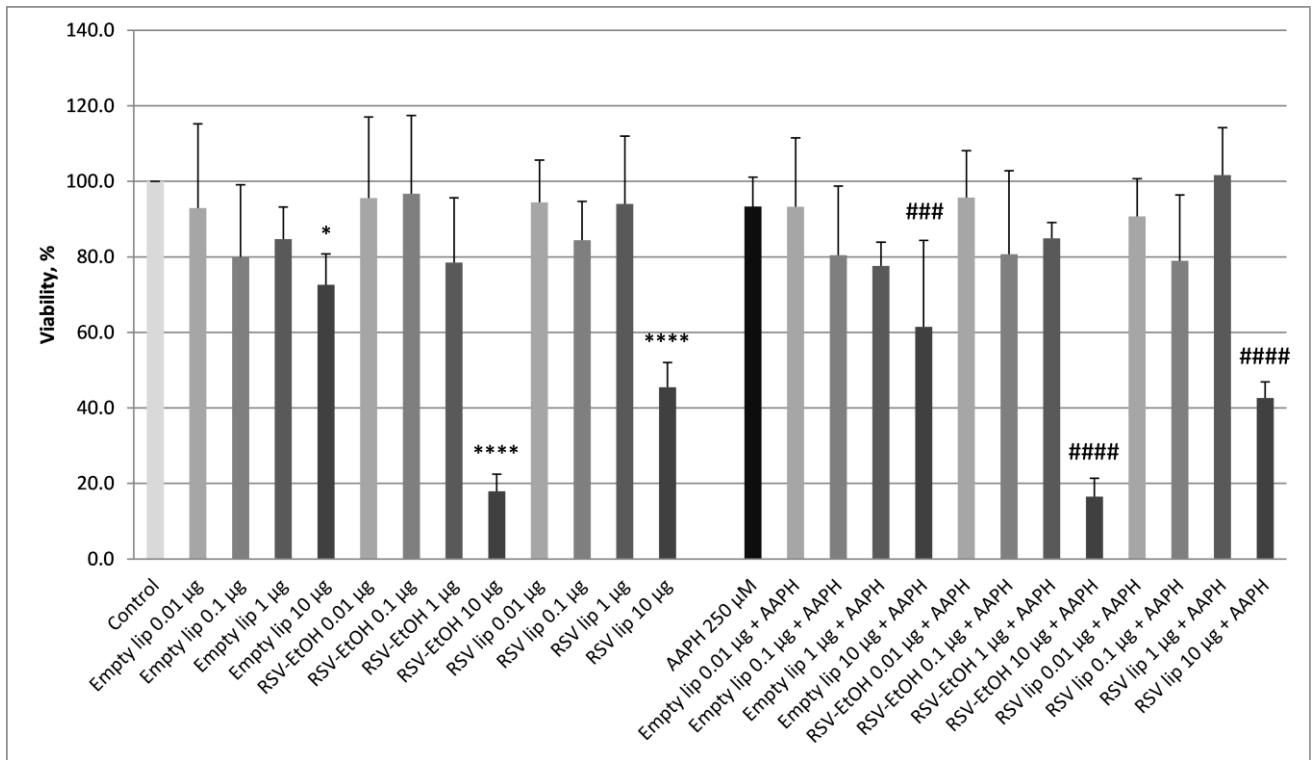
447

448



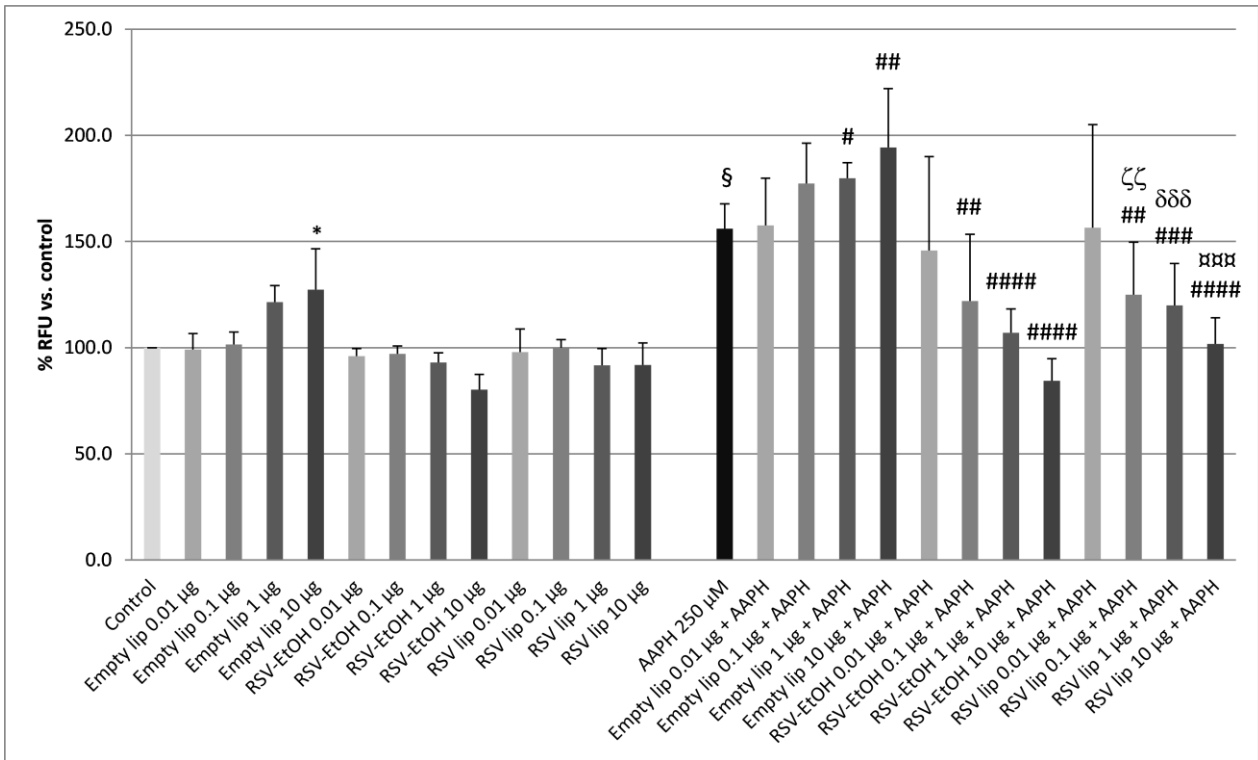
449

450



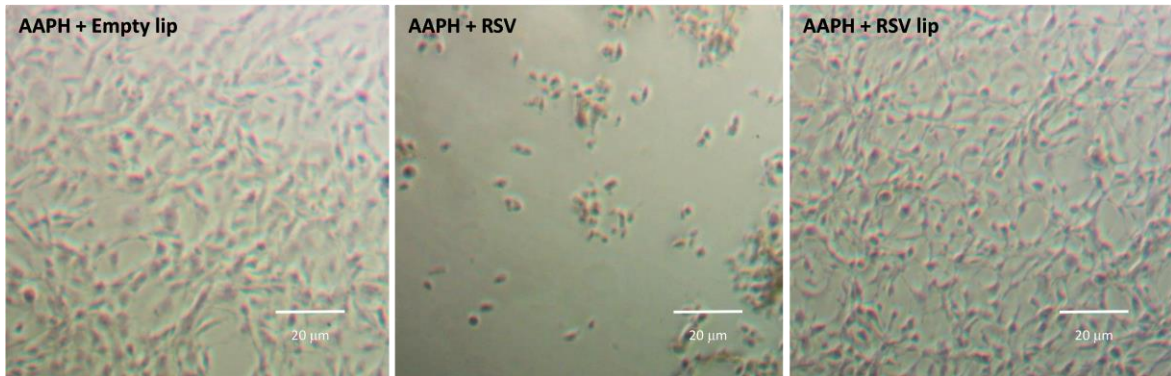
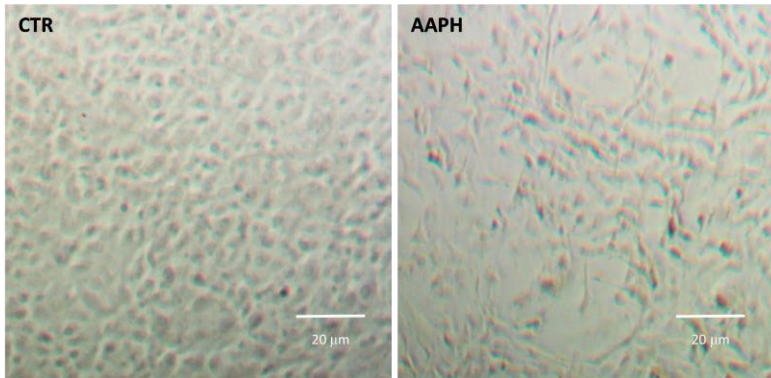
451

452



453

454



455

456

457

458 **Table 1.** Composition of the liposomal formulations.

Formulation	LIPO-N	RSV	Tween80	H₂O
Empty liposomes	100 mg		20 mg	2 ml
RSV liposomes	100 mg	4 mg	20 mg	2 ml

459

460

461 **Table 2.** Characteristics of empty and resveratrol (RSV) liposomes: mean diameter (MD),
 462 polydispersity index (PI), zeta potential (ZP), and entrapment efficiency (E). Each value represents
 463 the mean \pm SD ($n \geq 6$). * values statistically different ($p < 0.05$) from empty liposomes.

Formulation	MD nm \pm SD	PI	PZ mV \pm SD	E % \pm SD
Empty liposomes	82 \pm 4.4	0.22 \pm 0.02	-25 \pm 3.2	--
RSV liposomes	80 \pm 7.2	*0.19 \pm 0.02	-24 \pm 3.2	83 \pm 4.3

464

465

466 **Table 3.** *In vitro* antioxidant activity of resveratrol in the vesicle formulations in comparison with a
 467 methanolic solution. DPPH results are expressed as AA (%) and as TEAC ($\mu\text{g/ml}$) concentration.
 468 FRAP results are expressed as FE ($\mu\text{g/ml}$) concentration. Results are reported as the mean value \pm
 469 SD of 3 separate experiments, each performed in triplicate.

Formulation	DPPH		FRAP
	AA (%)	TEAC (μg of Trolox equivalents/ml)	FE (μg of Fe²⁺ equivalents/ml)
RSV in MeOH	87 \pm 2.5	325 \pm 3.3	8.8 \pm 1.0
Empty liposomes	8 \pm 1.6	165 \pm 23	0.2 \pm 0.002
RSV liposomes	84 \pm 1.4	321 \pm 7.0	8.1 \pm 0.7

470